

# Resistance of Poly(ethylene oxide)–Silane Monolayers to the Growth of Polyelectrolyte Multilayers

Cédric C. Buron, Vincent Callegari, Bernard Nysten, and Alain M. Jonas\*

Unité de Chimie et de Physique des Hauts Polymères (POLY), Université Catholique de Louvain (UCL), Croix du Sud 1, B-1348 Louvain-la-Neuve, Belgium (EU)

Received April 11, 2007. In Final Form: July 4, 2007

The ability of poly(ethylene oxide)–silane (PEO–silane) monolayers grafted onto silicon surfaces to resist the growth of polyelectrolyte multilayers under various pH conditions is assessed for different pairs of polyelectrolytes of varying molar mass. For acidic conditions (pH 3), the PEO–silane monolayers exhibit good polyelectrolyte repellency provided the polyelectrolytes bear no moieties that are able to form hydrogen bonds with the ether groups of the PEO chains. At basic pH, PEO–silane monolayers undergo substantial hydrolysis leading to the formation of negatively charged defects in the monolayers, which then play the role of adsorption sites for the polycation. Once the polycation is adsorbed, multilayer growth ensues. Because this is defect-driven growth, the multilayer is not continuous and is made of blobs or an open network of adsorbed strands. For such conditions, the molar mass of the polyelectrolyte plays a key role, with polyelectrolyte chains of larger molar mass adsorbing on a larger number of defects, resulting in stronger anchoring of the polyelectrolyte complex on the surfaces and faster subsequent growth of the multilayer. For polyelectrolytes of sufficiently low molar mass at pH 9, the growth of the multilayer can nevertheless be prevented for as much as five cycles of deposition.

## Introduction

The layer-by-layer (LbL) assembly of charged and H-bonding polymers, which consists of the cyclic adsorption of chains capable of complexing, is a standard method providing access to functional stratified films.<sup>1–8</sup> Among the main reasons for the current strong interest in LbL technology are the simplicity, versatility, limited cost, and environmental friendliness of this method. For some applications such as biosensors and photo- or electroactive devices, the controlled deposition of LbL assemblies in micro- or nanometer-sized regions is highly desirable. This can be done in different ways,<sup>9–29</sup> including adsorption on templates made

of patterned monolayers. For instance, we recently reported on the growth of multilayers in dots and lines of 20 to 200 nm size.<sup>29</sup> This was realized by performing LbL deposition on nanometer-sized hydrophobic regions drawn on a hydrophilic background. Apart from the interesting effects arising from the confinement of chains to spots smaller than their unperturbed dimensions in solution,<sup>29</sup> the ability to control LbL on this scale paves the way for the fabrication of soft structured surfaces integrating a high density of functional elements. For such applications, however, a crucial point is to produce monolayers capable of resisting the adsorption of a variety of polyelectrolytes for a given number of deposition cycles, typically five,<sup>29</sup> thereby forcing LbL to occur at the desired locations only.

Patterned surfaces showing polyelectrolyte repellency have been achieved by using monolayers consisting of short grafted chains of poly(ethylene oxide) (PEO).<sup>9–11,16,29</sup> PEO has been known to provide surfaces that resist protein adsorption<sup>30–33</sup> and is therefore frequently used to prepare biosensors.<sup>34</sup> However, the transposition of this concept to polyelectrolyte repellency is not direct; for instance, it was reported that PEO monolayers do not resist the adsorption of polyions of high molar mass<sup>10</sup> and that pH and ionic strength strongly modulate their polyelectrolyte repellency.<sup>11,16</sup> In our previous work on the nanometer scale,<sup>29</sup> we found adequate deposition conditions for a specific pair of polyelectrolytes, but the direct transposition of these conditions to other polyelectrolytes proved to be difficult, indicating that

\* Corresponding author. E-mail: alain.jonas@uclouvain.be.

- (1) Lvov, Y. M.; Decher, G. *Crystallogr. Rep.* **1994**, *39*, 628.
- (2) Decher, G. *Science* **1997**, *277*, 1232.
- (3) Bertrand, P.; Jonas, A.; Laschewsky, A.; Legras, R. *Macromol. Rapid Commun.* **2000**, *21*, 319.
- (4) Hammond, P. T. *Curr. Opin. Colloid Interface Sci.* **2000**, *4*, 430.
- (5) Decher, G.; Schlenoff, J., Eds. *Multilayer Thin Films*; Wiley: Weinheim, Germany, 2003.
- (6) Schönhoff, M. *J. Phys.: Condens. Matter* **2003**, *15*, R1781.
- (7) Arys, X.; Jonas, A. M.; Laschewsky, A.; Legras, R. In *Supramolecular Polymers*, 2nd ed.; Ciferri, A., Ed.; Marcel Dekker: New York, 2005; p 651.
- (8) Klitzing, R. v. *Phys. Chem. Chem. Phys.* **2006**, *8*, 5012.
- (9) Hammond, P. T.; Whitesides, G. M. *Macromolecules* **1995**, *28*, 7569.
- (10) Clark, S. L.; Montague, M.; Hammond, P. T. *Supramol. Sci.* **1997**, *4*, 141.
- (11) Clark, S. L.; Montague, M. F.; Hammond, P. T. *Macromolecules* **1997**, *30*, 7237.
- (12) Clark, S. L.; Hammond, P. T. *Adv. Mater.* **1998**, *10*, 1515.
- (13) Clark, S. L.; Handy, E. S.; Rubner, M. F.; Hammond, P. T. *Adv. Mater.* **1999**, *11*, 1031.
- (14) Jiang, X. P.; Hammond, P. T. *Langmuir* **2000**, *16*, 8501.
- (15) Chen, K. M.; Jiang, X. P.; Kimerling, L. C.; Hammond, P. T. *Langmuir* **2000**, *16*, 7825.
- (16) Clark, S. L.; Hammond, P. T. *Langmuir* **2000**, *16*, 10206.
- (17) Hua, F.; Shi, J.; Lvov, Y.; Cui, T. *Nano Lett.* **2002**, *2*, 1219.
- (18) Hua, F.; Cui, T.; Lvov, Y. *Langmuir* **2002**, *18*, 6712.
- (19) Cao, T.; Wei, F.; Jiao, X.; Chen, J.; Liao, W.; Zhao, X.; Cao, W. *Langmuir* **2003**, *19*, 8127.
- (20) Jaber, J. A.; Chase, P. B.; Schlenoff, J. B. *Nano Lett.* **2003**, *3*, 1505.
- (21) Pallandre, A.; Glinel, K.; Jonas, A. M.; Nysten, B. *Nano Lett.* **2004**, *4*, 365.
- (22) Doh, J.; Irvine, D. J. *J. Am. Chem. Soc.* **2004**, *126*, 9170.
- (23) Reyes, D. R.; Perruccio, E. M.; Becerra, S. P.; Locascio, L. E.; Gaitan, M. *Langmuir* **2004**, *20*, 8805.
- (24) Park, J.; Hammond, P. T. *Adv. Mater.* **2004**, *16*, 520.
- (25) Hammond, P. T. *Adv. Mater.* **2004**, *16*, 1271.

- (26) Shi, F.; Wang, Z.; Zhao, N.; Zhang, X. *Langmuir* **2005**, *21*, 1599.
- (27) Park, J.; Fouche, L. D.; Hammond, P. T. *Adv. Mater.* **2005**, *17*, 2575.
- (28) Olugebefola, S. C.; Ryu, S.-W.; Nolte, A. J.; Rubner, M. F.; Mayes, A. M. *Langmuir* **2006**, *22*, 5958.
- (29) Pallandre, A.; Moussa, A.; Nysten, B.; Jonas, A. M. *Adv. Mater.* **2006**, *18*, 481.
- (30) Golander, C.-G.; Herron, J. N.; Lim, K.; Claesson, P.; Stenius, P.; Andrade, J. D. In *Poly(Ethylene Glycol) Chemistry: Biotechnical and Biomedical Applications*; Harris, J. M., Ed.; Plenum Press: New York, 1992; pp 221–245.
- (31) Prime, K. L.; Whitesides, G. M. *J. Am. Chem. Soc.* **1993**, *115*, 10714.
- (32) Holmberg, K.; Tiberg, F.; Malmsten, M.; Brink, C. *Colloids Surf., A* **1997**, *123*, 297.
- (33) Zhang, M.; Desai, T.; Ferrari, M. *Biomaterials* **1998**, *19*, 953.
- (34) Sharma, S.; Johnson, R. W.; Desai, T. A. *Biosens. Bioelectron.* **2004**, *20*, 227.

further studies on the polyelectrolyte repellency of PEO-based surfaces were required.

Previous work on polyelectrolyte-repellent surfaces was carried out on PEO-terminated thiol monolayers self-assembled onto gold surfaces. However, no study has been reported regarding the polyelectrolyte repellency of monolayers of PEO-silane grafted onto silicon substrates. PEO-silane silicon oxide surfaces have been reported to exhibit excellent protein repellency.<sup>35–37</sup> However, such surfaces may exhibit significantly different behavior toward polyelectrolytes than do previously studied PEO-thiol monolayers because their grafting density is usually lower than that of thiols assembled on gold and because their hydrolytic stability is rather different. Therefore, here we examine the repellency properties of PEO-silane monolayers toward the growth of polyelectrolyte multilayers. The repellency is evaluated by analyzing the surface after five cycles of (polycation/polyanion) adsorption. Different pairs of polyelectrolytes of varying molar masses are tested under different pH conditions, and a range of techniques are applied to elucidate the growth of multilayers on the PEO-modified silicon surfaces (ellipsometry, X-ray reflectometry, X-ray photoelectron spectroscopy, and atomic force microscopy).

### Experimental Section

**Materials.** One-side-polished 475- $\mu\text{m}$ -thick Si(100) wafers were purchased from ACM (Applications Couches Minces, France). 2-Methyl(polyethyleneoxy)propyl-trichloro-silane (PEO-silane,  $M_w = 426\text{--}558\text{ g/mol}$ ) was obtained from Gelest (Germany). Toluene (extra dry,  $[\text{H}_2\text{O}] < 30\text{ ppm}$ ), dichloromethane (HPLC grade), and ethanol were obtained from Acros Organics. Sulfuric acid (98%) and hydrogen peroxide (30%) were from Merck VWR. Poly(diallyldimethylammonium chloride) (PDDA), poly(styrene sodium sulfonate) (PSS), and poly(acrylic acid) (PAA) were purchased from Aldrich; poly(vinylbenzyl chloride) quaternized with *N,N*-dimethylethanolamine (PVBAC) was prepared as described elsewhere.<sup>38</sup> Different molar masses of PAA and PDDA were used (PAA:  $M_w = 5100, 15\,000, 100\,000, 250\,000$ ; PDDA:  $M_w < 10^5, 10^5\text{--}2 \times 10^5, 4 \times 10^5\text{--}5 \times 10^5$ ), whereas PSS and PVBAC had average molar masses by weight ( $M_w$ ) of 75 000 and 84 000.<sup>39</sup>

**Preparation of Oligo(ethylene) Oxide Monolayers on Silicon.** Prior to functionalization, silicon substrates were cleaned in piranha solution (3:1 v/v 98%  $\text{H}_2\text{SO}_4$ /30%  $\text{H}_2\text{O}_2$ ) maintained at 70 °C for 25 min. After extensive rinsing with ultrapure water (Milli-Q water obtained from a Millipore system with a resistivity larger than 18.2  $\text{M}\Omega\cdot\text{cm}$ ), the wafers were spin dried and immersed in a fresh 20 mM solution of PEO-silane in dry toluene for 6 h, giving rise to a monolayer of high grafting density.<sup>37</sup> The silanation was performed in a glove box with a moisture level below 0.5 ppm. The substrates were then washed in a dichloromethane Soxhlet for 24 h before being sonicated for 5 min in ethanol. The wafers were finally rinsed with ultrapure water and dried with nitrogen.

**Deposition of Polyelectrolyte Multilayers.** The PEO-silane wafers were dipped alternatively into cationic and anionic polyelectrolyte solutions for 5 min, starting from the polycation solution. The concentration of the polyelectrolyte solutions was 0.01 M in repeat units. To remove nonadsorbed macromolecules, the wafers were rinsed three times between each adsorption step by dipping them into water of the same pH as the polyelectrolyte solution. The pH of the solutions was adjusted by the addition of small amounts of NaOH or HCl. The detailed rinsing procedure is as follows: fifteen 1 s dips in the first rinsing bath, followed by ten 1 s dips in the

second rinsing bath and then by one 2 min dip in the third rinsing bath. Five cycles of immersion were performed to evaluate the polyelectrolyte repellency of PEO-silane monolayers.

**Ellipsometry.** A Digisil rotating compensator, single-wavelength ellipsometer from Jobin Yvon/Sofie Instruments was employed to follow the growth of the films. This instrument is equipped with a helium-neon laser working at 632.8 nm. To minimize some systematic errors such as imperfections and residual misalignment, measurements were performed with the analyzer set at +45° and -45°. The film thickness was extracted from a fit of the  $\Psi$  and  $\Delta$  values (ellipsometric angles) using a model composed of a flat substrate coated with an isotropic film.<sup>40</sup> The refractive indices were fixed to 3.881- $j$ 0.019 and 1.47 for the silicon substrate<sup>41</sup> and the adsorbed layer, respectively. This latter value is in the range of refractive indexes of polymers<sup>42</sup> and is close to values typically encountered in the literature.<sup>43,44</sup> Because the indices of refraction of silicon dioxide and organic materials are close together, the layer of native oxide atop the silicon wafer could not be distinguished by ellipsometry from the layer of grafted and adsorbed organic material. Consequently, the thickness of the native oxide layer ( $\sim 1.5\text{ nm}$  measured by ellipsometry on a series of bare wafers, just after cleaning) was removed from the ellipsometric thickness of the film to obtain the thickness of the organic film. For some samples, the roughness and porosity of the films were so high that the thickness derived from ellipsometry is meaningless. In that case, the ellipsometric thickness should be taken as the thickness of a continuous equivalent film of the same adsorbed amount as in the real, imperfect sample, as demonstrated at the end of the article.

**X-ray Photoelectron Spectroscopy (XPS).** XPS analysis was carried out with an SSX-ESCA 300 photoelectron spectrometer (Surface Science Instruments) with a monochromatic Al K $\alpha$  X-ray source (1486.6 eV). The photoelectron takeoff angle (TOA) was 55°, and the energy resolution was set to 1.4 eV. The energy calibration of the spectra was done by setting the Si 2p core level to 99.4 eV.<sup>45</sup> The quantification of detected elements was performed on the basis of the areas of their associated photoemission peak normalized by the elemental sensitivity factors of the spectrometer.

**Atomic Force Microscopy (AFM).** A Nanoscope IV from Veeco Instruments (Santa Barbara, CA) was used in air in intermittent contact (or tapping) mode (IC-AFM) to investigate the surface morphology. The silicon cantilevers (PointProbe Tapping-mode cantilevers from Nanosensors) that we used had a resonance frequency of around 160–165 kHz with a typical spring constant of around 40 N/m and an integrated silicon tip with an apex radius of curvature lower than 10 nm as stated by the manufacturer.

**X-ray Reflectometry (XRR).** The XRR measurements were carried out with a modified Siemens D5000 2-circle goniometer fitted to a Rigaku rotating anode operated at 40 kV and 300 mA, delivering Cu K $\alpha$  radiation of 0.15418 nm wavelength. Monochromatization and collimation were achieved with the help of a collimating curved multilayered mirror (Osmic, Japan), delivering a close-to-parallel beam of about 0.0085° angular divergence. The beam size was defined by a 40- $\mu\text{m}$ -wide slit. The intensity was scaled to unit incident intensity and corrected for spill over at very low angles of incidence. The reflectograms are reported as a function of the vertical component of the wavevector of the incident photons in a vacuum,  $k_{z0} = (2\pi/\lambda)\sin\theta$  where  $\lambda$  is the X-ray wavelength and  $\theta$  is half of the scattering angle. From the XRR data, an estimation of the average thickness of the deposited film,  $d$ , was obtained from the location of the first minimum in the reflectivity

(40) Azzam, R. M. A.; Bashara, N. M. *Ellipsometry and Polarized Light*; North Holland: Amsterdam, 1977.

(41) Aspnes, D. E.; Studna, A. A. *Phys. Rev.* **1983**, 27, 985.

(42) Seferis, J. C. In *Polymer Handbook*, 3rd ed.; Brandrup, J., Immergut, E. H., Eds.; John Wiley & Sons: New York, 1989; pp VI/451–VI/461.

(43) Schwarz, S.; Eichhorn, K. J.; Wischerhoff, E.; Laschewsky, A. *Colloids Surf., A* **1999**, 159, 491.

(44) Buron, C. C.; Membrey, F.; Filiâtre, C.; Foissy, A. *Colloids Surf., A* **2006**, 289, 163.

(45) Moulder, J. F.; Stickle, W. F.; Sobol, P. E.; Bomben, K. D. *Handbook of Photoelectron Spectroscopy*; Perkin-Elmer Corporation, Physical Electronics Division: Eden Prairie, MN, 1992.

(35) Lee, S.-W.; Laibinis, P. E. *Biomaterials* **1998**, 19, 1669.

(36) Papra, A.; Gadegaard, N.; Larsen, N. B. *Langmuir* **2001**, 17, 1457.

(37) Cecchet, F.; De Meersman, B.; Demoustier-Champagne, S.; Nysten, B.; Jonas, A. M. *Langmuir* **2006**, 22, 1173.

(38) Nicol, E.; Habib-Jiwan, J.-L.; Jonas, A. M. *Langmuir* **2003**, 19, 6178.

(39) Alem, H.; Blondeau, F.; Glinel, K.; Demoustier-Champagne, S.; Jonas, A. M. *Macromolecules* **2007**, 40, 3366.

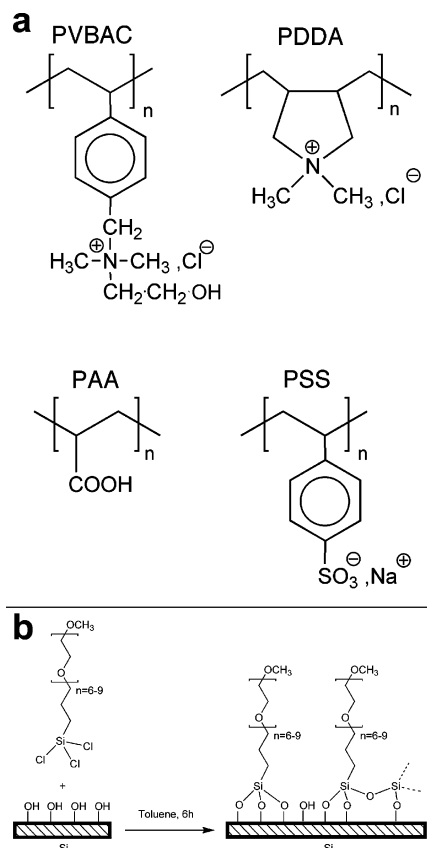


**Figure 1.** (a) Chemical structures of the polyelectrolytes in this study. (b) Schematic drawing of the fabrication of the PEO-silane monolayers.

curve,  $k_{Z0, \min}$ . For a thin organic film (below 4 nm thickness), this minimum, which originates from the destructive interference between the beam reflected at the upper and lower interfaces of the film, is related to the film thickness by the approximate relationship  $d = \pi/2k_{Z0, \min}$ . In addition to this simple estimation of thickness, a more thorough analysis of the reflectograms was performed that involved the fit of electron density profiles as described previously.<sup>37,46</sup>

## Results and Discussion

Data on the deposition of multilayers on silicon wafers are given in this opening section because they serve as a reference in the sequel. The selected polyelectrolytes are shown in Figure 1a. They include two strong pH-insensitive polycations, poly(vinylbenzyl chloride) quaternized with *N,N*-dimethylethanolamine (PVBAC) and poly(diallyl dimethyl ammonium chloride) (PDDA), a pH-insensitive strong polyanion, poly(styrene sodium sulfonate) (PSS), and a pH-sensitive polyanion, poly(acrylic acid) (PAA). This selection allows us to tune the relative strength of electrostatic and H-bonding interactions in the multilayers. This tuning can also be performed by adjusting the pH of the solutions, which was set at fixed values between 3 and 9 to ensure that the increase in ionic strength resulting from the addition of base or acid is negligible in comparison with the intrinsic ionic strength resulting from the polyelectrolytes themselves. Unless otherwise noted, the thickness and morphology of the films were recorded after five cycles of deposition. This specific number of cycles was chosen in part because it allows us to amplify small adsorption events that would not be noticed after only one cycle of deposition.

Bare silicon wafers are covered by a layer of native oxide of about 1.5 nm thickness, which has an isoelectric point of around pH 2 and is thus negatively charged above this pH value.<sup>47,48</sup> For

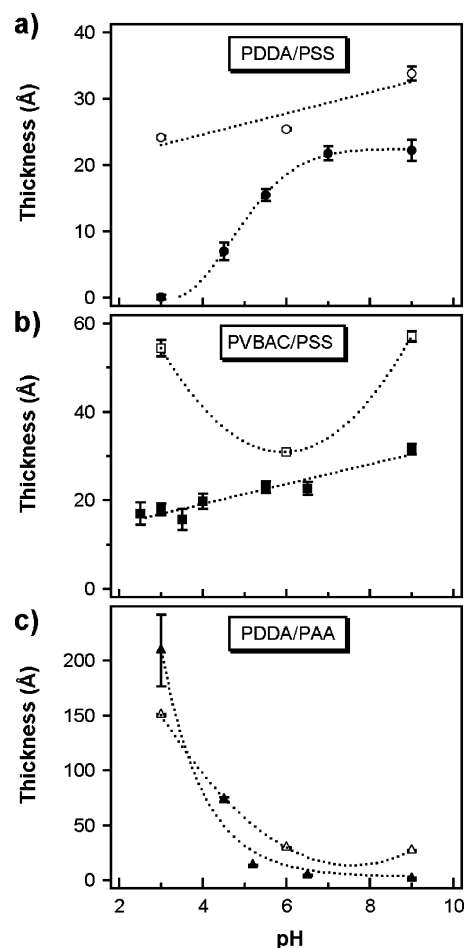


**Figure 2.** Thickness of polyelectrolyte multilayers grown for five cycles on bare silicon wafers (open symbols) or PEO-silane wafers (closed symbols) from solutions of varying pH. (a) (PDDA/PSS)<sub>5</sub>, (b) (PVBAC/PSS)<sub>5</sub>, and (c) (PDDA/PAA)<sub>5</sub>. The average molar mass by weight of the PAA used in these experiments is 15 000, and that for PDDA is  $10^5$ – $2 \times 10^5$ . The thickness shown is the difference between the total thickness of the organic film and the thickness of bare PEO-silane monolayers as measured by ellipsometry.

multilayers based on strong polyions PDDA and PSS, which cannot engage in H bonding, the thickness recorded on silicon after five deposition cycles increases with pH (Figure 2a, open symbols). Previous work on the adsorption of strong polyelectrolytes on oxides have shown a similar dependence of the adsorbed amount on pH, resulting from the enhancement of surface charge by adsorbing polyelectrolytes.<sup>48</sup> When PDDA is replaced by PVBAC (Figure 2b, open symbols), the thickness of the multilayer also increases at lower pH. This is due to the protonation of the layer of native silicon oxide that starts below pH 4, resulting in the formation of surface Si–OH groups that engage in significant hydrogen bonding with the hydroxyl groups of PVBAC, thereby increasing the initially adsorbed amount of this polyelectrolyte. As for (PDDA/PAA)<sub>5</sub> multilayers grown on Si (Figure 2c, open symbols), they exhibit a strong pH-dependent thickness resulting from the varying charge density of PAA with pH, a phenomenon that has been amply documented since the publication of a seminal paper by Rubner et al.<sup>49</sup> As shown in Figure 2c, (PDDA/PAA) multilayers grow for pH values as low as 3. This is because the  $pK_a$  of PAA is considerably lowered

(47) Baudrant, A.; Tardif, F.; Wyon, C. *Caractérisation et Nettoyage du Silicium*; Éditions Lavoisier: Paris, 2003.

(48) Hooijveen, N. G.; Chen Stuart, M. A.; Fleer, G. J. *J. Colloid Interface Sci.* **1996**, 182, 133.

(49) Yoo, D.; Shiratori, S. S.; Rubner, M. F. *Macromolecules* **1998**, 31, 4309.

(46) Arys, X.; Laschewsky, A.; Jonas, A. M. *Macromolecules* **2001**, 34, 3318.



in (PDDA/PAA) complexes compared to that of free PAA, with about 10% of the acid groups of PAA being charged in the complexes at pH 3.<sup>50</sup> Although low, this degree of charge is certainly sufficient to grow multilayers in unsalted water in combination with a strongly charged polyelectrolyte, as was shown and rationalized by us before.<sup>51</sup>

#### Polyelectrolyte Repellency of PEO–Silane Wafers Depending on the Solution pH and Nature of the Polyelectrolyte.

Dense oligo(ethylene)oxide monolayers of about 1.5 nm thickness (XRR-determined value) were reproducibly obtained from 2-methyl(polyethyleneoxy)propyl-trichloro-silane (PEO–silane) using the silanation method described previously (Figure 1b).<sup>37</sup> Their polyelectrolyte repellency was tested as a function of solution pH and the nature of the polyelectrolyte. Figure 2a (closed symbols) presents the ellipsometry-derived thickness of (PDDA/PSS)<sub>5</sub> multilayers adsorbed on PEO–silane wafers versus the pH of the deposition and rinsing solutions. The PEO–silane wafers resist multilayer deposition at pH 3 but progressively lose their repellency as the solution pH increases, until a plateau of thickness is reached for the more basic pH values. Resistance to multilayer growth is thus limited to low pH values, even though the polyelectrolytes are pH-insensitive. When the polycation is changed from PDDA to PVBAC (Figure 2b, closed symbols), a completely different behavior emerges. Although the multilayers grow less than on silicon, they are nevertheless never prevented from growing by the PEO coating, with the film thickness increasing linearly from 17 Å at pH 3 to 32 Å at pH 9. Unsurprisingly, (PDDA/PAA)<sub>5</sub> multilayers show the same dramatic dependence of thickness on pH as observed on silicon, resulting from the pH dependence of the charge density of PAA. The PEO–silane wafers do not prevent (PDDA/PAA) multilayer growth except at higher pH 9, where the multilayer thickness tends to zero for the specific molar masses used in these experiments (PDDA:  $(1-2) \times 10^5$ ; PAA: 15 000; other molar masses are discussed later).

These experiments indicate that multilayer growth on PEO–silane monolayers strongly depends on the nature of the polyelectrolyte and the solution pH. Considering the structural differences between the tested polyelectrolytes, it is obvious that different types of interaction must be considered to explain the experimental observations. The first interaction that explains part of our results is hydrogen bonding. Rubner et al. were the first to demonstrate the possibility of building PEO-based multilayers by only using hydrogen bonding between the H-bond-accepting ether groups of PEO and a H-bond-donating polymer (in this case, polyaniline).<sup>52</sup> Subsequent work showed that PEO/PAA and PEO/poly(methyl methacrylic acid) hydrogen-bonded multilayers could be grown as well.<sup>53,54</sup> In the present case, the repeat units of both PVBAC and PAA exhibit –OH groups that can hydrogen bond to the PEO–silane surface. Once PVBAC or PAA is absorbed on the PEO–silane surface, multilayers of PVBAC/PSS or PDDA/PAA can then be grown by standard electrostatic interaction. However, an important difference exists between PVBAC and PAA because the former is H-bond-donating irrespective of pH, whereas the H-bond-donating capabilities of the latter are restricted to the pH range where the carboxylic acid moieties are protonated. This explains why (PDDA/PAA) multilayers do not grow on the PEO–silane surfaces at pH 9, where the –COOH functions are fully deprotonated.

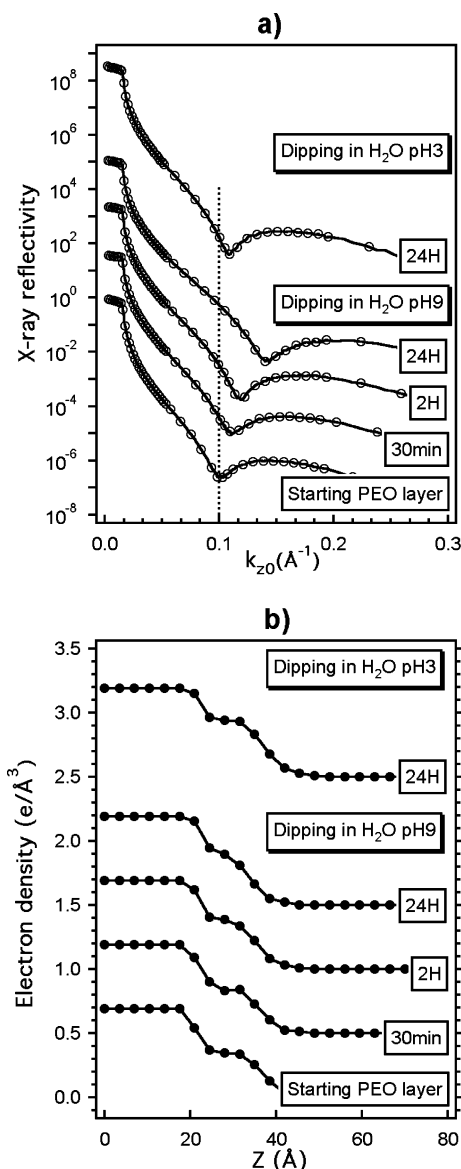


**Figure 3.** (a) X-ray reflectograms of PEO monolayers immersed for different times in water at pH 3 or 9. The vertical dashed line indicates the location of the first minimum (destructive interference) in the reflectograms of the original PEO–silane wafer. Only every fifth data point is shown in the graphs. (b) Corresponding electron density profiles. Circles correspond to computed densities whereas continuous lines were obtained by cubic spline interpolation.

For (PDDA/PSS) multilayers, H bonding cannot explain the observed multilayer adsorption at higher pH because these polyelectrolytes do not exhibit H-bond-donating moieties. Therefore, to elucidate the behavior of the PDDA/PSS system, the stability of the PEO–silane monolayers was investigated. The PEO layers were immersed in water at pH 3 and 9 for different times in the absence of polyelectrolyte, and their dry thickness was measured by X-ray reflectivity and ellipsometry after careful rinsing in neutral water to allow a meaningful comparison between samples. Figure 3a,b present the X-ray reflectograms of these monolayers and their computed electron density profiles, respectively. The first Kiessig fringe in the reflectograms of Figure 3a shifts with immersion time to higher  $k_{z0}$  values, which indicates a progressive decrease in layer thickness that is also visible in the computed electron density profiles of Figure 3b. The average film thicknesses obtained by XRR and ellipsometry, which are summed up in Table 1, confirm that the layer thickness decreases slowly in water, with the rate of decrease being faster

(50) Petrov, A. I.; Antipov, A. A.; Sukhorukov, G. B. *Macromolecules* **2003**, *36*, 10079.

(51) Glinel, K.; Moussa, A.; Jonas, A. M.; Laschewsky, A. *Langmuir* **2002**, *18*, 1408.

(52) Stockton, W. B.; Rubner, M. F. *Macromolecules* **1997**, *30*, 2717.

(53) Sukhishvili, S. A.; Granick, S. *Macromolecules* **2002**, *35*, 301.

(54) DeLongchamp, D. M.; Hammond, P. T. *Langmuir* **2004**, *20*, 5403.

**Table 1. Film Thickness of PEO–Silane Monolayers after Immersion in Water at Different pH Values**

immersion time (min)	$d_{\text{XRR}}$ (Å), pH 3 <sup>a</sup>	$d_{\text{ell}}$ (Å), pH 3 <sup>b</sup>	$d_{\text{XRR}}$ (Å), pH 9 <sup>a</sup>	$d_{\text{ell}}$ (Å), pH 9 <sup>b</sup>
0	15.1	15	15	14.9
30		14	13.5	13.4
120		13.6	12.6	12.4
1440	13.2	13	10.3	10.3

<sup>a</sup> Value determined from the location of the first Kiessig fringe in X-ray reflectograms. <sup>b</sup> Value determined by ellipsometry. The average standard error is 1.4 Å.

under basic conditions. This may be due to only the slow hydrolysis of Si–O siloxanes by hydroxide ions.<sup>55</sup> The hydrolysis results in the erosion of 13 and 30% of the film after 24 h of immersion in water at pH 3 and 9, respectively. Note that the hydrolysis slows down with time, suggesting that a distribution of bond strengths exists in the monolayer, probably as a result of the distribution in the number of condensed silanols per PEO–silane molecule. XPS was performed on the monolayers prior to water immersion and after 1440 min of immersion under both pH conditions. From the C 1s core-level photoemission spectra of PEO monolayers, the ratio between the number of ethylene oxide carbon atoms (at 286.4 eV) and the number of silicon atoms was computed. Directly after monolayer synthesis, a value of 37.5% is found for the C–O/Si ratio. Dipping for 1440 min in water at pH 3 and 9 induces a decrease in this ratio to 36.7 and 23%, respectively. The diminution of the C–O/Si ratio confirms the loss of PEO-grafted molecules due to Si–O hydrolysis, even though a direct quantitative comparison with ellipsometry is not possible given the limitations of the method. Furthermore, a marked difference in the hydrolysis rate is observed between acidic and basic conditions, as was also seen from the thickness variation, which is obviously related to strong variations in the concentration of hydroxyl ions depending on pH and possibly to the reported lower permeability of PEO monolayers to hydroxide ions below pH 4.<sup>13</sup>

Given the slow hydrolysis of the PEO–silane monolayer, it becomes possible to understand the peculiar dependence of the thickness of (PDDA/PSS)<sub>5</sub> multilayers on pH (Figure 2). The growth of a five-cycle multilayer takes about 1 h, during which time PEO–silane molecules chemisorb, thereby creating free Si–OH defects in the layer. At pH 3, hydrolysis is slow, and the freshly created silanol groups are protonated. Therefore, they do not interact electrostatically with PDDA or PSS, which results in the preservation of the polyelectrolyte repellency of the PEO–silane layer. At higher pH, hydrolysis is accelerated, and the created silanol groups are not protonated, thereby attracting some PDDA molecules to the surface. In turn, these molecules serve to attract PSS molecules, resulting in the progressive coverage of the surface by the multilayer and a loss of polyelectrolyte repellency.

**Influence of the PDDA Molar Mass on the Resistance of PEO–Silane Layers to the Growth of (PDDA/PSS) Multilayers.** Previous work by Hammond et al. on the antifouling properties of oligo(ethylene glycol)-terminated alkanethiol monolayers on gold showed that the higher the molar mass of the polyelectrolytes, the larger their adsorption on such layers.<sup>56,57</sup> Because this parameter could also be important to PEO–silane monolayers on Si, we investigated the growth of (PDDA/PSS)

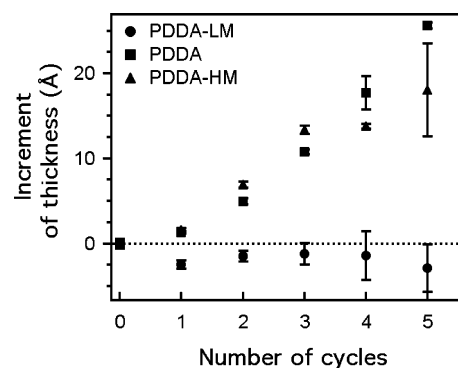


**Figure 4.** Thickness increment of a PEO–silane monolayer for different numbers of deposition cycles of (PDDA/PSS) at pH 9. The increment is defined here as the difference between the total film thickness after a given number of deposition cycles and the original thickness of the PEO layer. Different molar masses of PDDA were tested (●, PDDA of  $M_w < 10^5$ ; ■, PDDA of  $M_w = 10^5$ – $2 \times 10^5$ ; ▲, PDDA of  $M_w = 4 \times 10^5$ – $5 \times 10^5$ ), and the molar mass of PSS was kept constant at  $M_w = 70\,000$ . A negative increment value indicates partial hydrolysis of the PEO layer.

**Table 2. Nitrogen/Silicon and Sulfur/Silicon Ratios Measured by XPS on PEO–Silane Monolayers Immersed for 5 min in Different Polyelectrolyte Solutions (pH 9)**

polyelectrolyte	N/Si (%)	S/Si (%)
PDDA-LM, $M_w < 10^5$	2.4	0
PDDA, $M_w = 10^5$ – $2 \times 10^5$	2.7	0
PDDA-HM, $M_w = 4 \times 10^5$ – $5 \times 10^5$	3.4	0
PSS, $M_w = 7 \times 10^4$	0	0

multilayers on PEO–silane monolayers using three commercially available PDDAs. The PDDA used so far is reported to have an average molar mass by weight,  $M_w$ , of  $10^5$ – $2 \times 10^5$ , a low molar mass sample (PDDA-LM,  $M_w < 10^5$ ), and a high molar mass sample (PDDA-HM,  $M_w = 4 \times 10^5$ – $5 \times 10^5$ ). Figure 4 presents the increment of thickness of the organic layer versus the number of cycles of PDDA/PSS deposition at pH 9. Whereas the multilayers based on both the standard and high molar mass PDDA increase similarly in thickness with the number of deposition cycles, the multilayers based on the low molar mass PDDA fail to grow on the PEO–silane layer. In this case, the slight decrease in thickness reported in Figure 4 is due to the limited hydrolysis of the PEO–silane layer during the immersion cycles.

To identify the polyelectrolyte that is first adsorbed onto the PEO monolayer, XPS measurements were performed on samples dipped once either in one of the PDDA solutions or in the PSS solution and then rinsed in water at pH 9. No trace of sulfur could be found on the PEO–silane wafers after dipping in the PSS solution, indicating that the PEO monolayers resist the adsorption of the polyanion. By contrast, significant amounts of nitrogen were found on the PEO monolayers after immersion in any of the three PDDA solutions (Table 2), indicating that PDDA adsorption is the step from which the growth of the multilayer starts. As stated above, the adsorption of the polycation most probably originates from electrostatic interaction between the positive charges of PDDA and the negative charges of surface silanols, which are ionized at pH 9. These silanol groups result in part from the hydrolysis of the PEO layer as demonstrated in the previous section but may also be due to nonreacted silanols that are known to exist after silanation.<sup>58</sup>

Interestingly, the PDDA sample of low molar mass is also found to adsorb on the PEO monolayer, although no subsequent

(55) Iler, R. K. *The Chemistry of Silica: Solubility, Polymerization, Colloid and Surface Properties and Biochemistry*; John Wiley & Sons: New York, 1979.

(56) Clark, S. L.; Montague, M.; Hammond, P. T. *Supramol. Sci.* **1997**, *4*, 141.

(57) Clark, S. L.; Montague, M. F.; Hammond, P. T. *Macromolecules* **1997**, *30*, 7237.

(58) Wasserman, S. R.; Tao, T. Y.; Whitesides, G. M. *Langmuir* **1989**, *5*, 1074.

multilayer growth occurs with this polymer. Compared to long PDDA chains, short PDDA chains are less strongly adsorbed to the PEO monolayers because they may bind to only a limited number of defect sites in the monolayer and because their entropy is more severely decreased upon adsorption. Therefore, they are more easily displaced by PSS in the next step of the deposition cycle, forming a soluble complex in solution similarly to what was proposed by Cohen Stuart et al. for weakly charged polyelectrolytes.<sup>59</sup> When similar experiments were conducted at pH 3, no variation of thickness was observed, and no nitrogen peak could be observed by XPS whatever the molar mass of PDDA. These results corroborate the fact that the PEO-silane monolayers are effective at preventing PDDA/PSS multilayer adsorption at acidic pH, a condition for which the silanol groups are not ionized and at which hydrolysis of the silane monolayer is moderate.

**Influence of the Molar Mass of PDDA and PAA on the Resistance of PEO-Silane Layers to the Growth of (PDDA/PAA) Multilayers.** As stated above, PEO-silane layers resist the growth of (PDDA/PSS) multilayers at acidic pH whatever the molar mass of PDDA. They were also found to resist the growth of (PDDA/PAA) multilayers at basic pH (Figure 2b) for a PDDA of medium molar mass ( $1 \times 10^5$ – $2 \times 10^5$ ) and a PAA of 15 000 molar mass. Therefore, to further explore the role of the polyelectrolyte chain length in the repellency of PEO-silane monolayers, we investigated the growth of such multilayers at pH 9, where the molar mass of both PDDA and PAA was systematically varied (Figure 5). After one cycle of deposition, a strong decrease in thickness is observed for all tested molar masses. This decrease is much larger than the one observed when the PEO-silane layer is immersed in water at pH 9 in the absence of polyelectrolytes. This suggests that polyelectrolyte adsorption may affect the rate of hydrolysis of the siloxane moieties, possibly because of the complexation and displacement of loosely bound or hydrolyzed silane molecules by the polyelectrolytes in solution. Conformational changes in the PEO layer due to complexation with  $\text{Na}^+$  cations (from the NaOH used to tune the pH) and the trapping of these changes following adsorption of the polyelectrolytes might also be considered to explain the observed larger decrease in thickness.

When larger numbers of deposition cycles are used, the growth of multilayers occurs progressively, with the general trend being that the larger the molar mass of either PAA or PDDA, the larger the thickness increment. It was shown before that PDDA adsorbs onto the PEO-silane wafers at pH 9. Apparently, this is sufficient in most cases to start multilayer growth, although using PAA and PDDA of low molar masses may delay multilayer growth to more than five cycles. The reason for this behavior is similar to that proposed for the (PDDA/PSS) multilayers of the previous section, which is related to the existence of an equilibrium between soluble and insoluble complexes on the surface of the multilayer. The use of polyelectrolytes of lower mass favors the solubility of the complexes because of the limited number of stitching points on the surface; as a result, multilayer growth is delayed in inverse proportion to the molar masses of both the polycation and the polyanion. Thus, the polyelectrolyte repellency of the PEO layer is limited to the combination of polyelectrolytes of low molar masses and fails dramatically for longer chains.

**Structure of PEO-Silane Layers after Multilayer Deposition.** AFM measurements were performed in tapping mode on the PEO-silane wafers before and after multilayer deposition using conditions where the PEO-silane layer does not resist

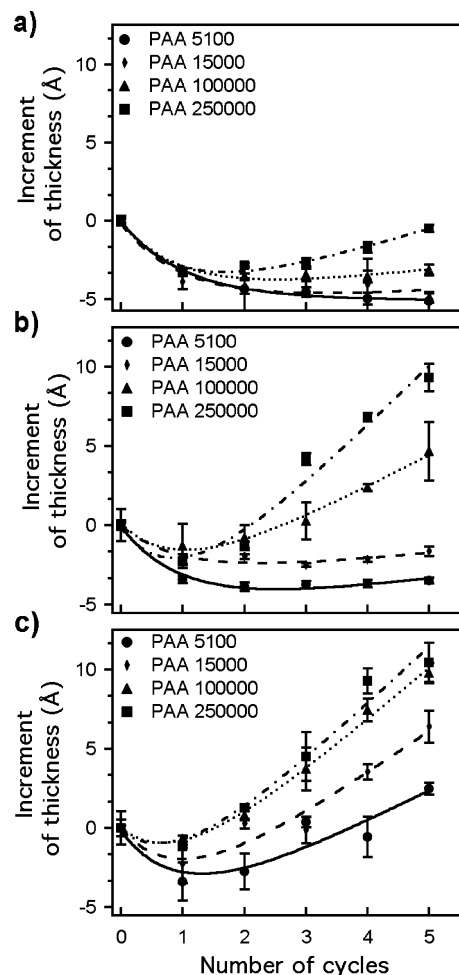


**Figure 5.** Increment of thickness of a PEO-silane monolayer for different numbers of deposition cycles of (PDDA/PAA) at pH 9. Different molar masses of PAA were used as indicated. (a–c) PDDA's of  $M_w = 10^5$ ,  $10^5$ – $2 \times 10^5$ , and  $4 \times 10^5$ – $5 \times 10^5$ , respectively. A negative increment value indicates partial hydrolysis of the PEO layer.

adsorption. Before multilayer growth, the PEO monolayer surfaces are uniform, having a root-mean-square (rms) roughness ( $R_{\text{rms}}$ ) of 3.2–3.6 Å (calculated on surfaces of  $2 \times 2 \mu\text{m}^2$ ) that is close to that of bare silicon (Figure 6a), confirming the XRR results showing the PEO-silane grafts as a homogeneous monolayer (Figure 3). Figure 6b–f shows the morphology of various multilayers adsorbed on the PEO layer. In all cases, the multilayers are discontinuous, being formed of blobs or an open network of adsorbed material showing that, even under these conditions, the PEO-silane layer provides partial resistance to multilayer growth. However, the growth is not prevented from starting from specific locations, most probably from sufficiently large defects in the layer as a result of partial hydrolysis (or collections of defects), which results in the formation of a discontinuous film if the average distance between such defects is large compared to typical chain dimensions. It is thus obvious that, provided a sufficient number of cycles is used, the surface will ultimately be fully covered by polyelectrolytes; however, a larger number of cycles will usually be required to reach a given film thickness as compared to that for standard non-polyelectrolyte-attracting surfaces. These AFM results thus provide strong support for a model of multilayer growth from defect sites, which is in good agreement with the observation that multilayer growth is favored for polyelectrolytes of larger molar mass.

(59) Hoogeveen, N. G.; Cohen Stuart, M. A.; Fleer, G. J. *Langmuir* **1996**, *12*, 3675.



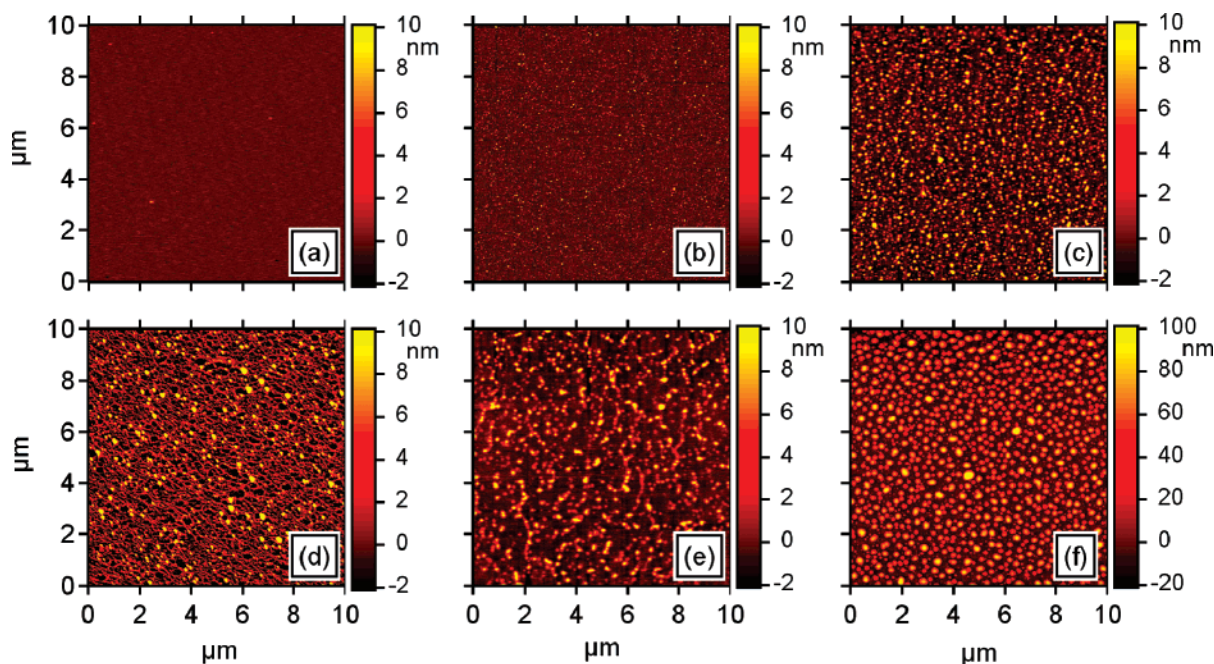


**Figure 6.** AFM topographic images of (a) a bare PEO monolayer and (b–f) a PEO monolayer onto which various multilayers were grown (five deposition cycles). (b) PVBAC/PSS grown at pH 9, (c) PDDA-HM/PAA grown at pH 9 ( $M_w$  of PAA is  $10^5$ ), (d) PDDA-HM/PSS grown at pH 9, (e) PDDA-LM/PSS grown at pH 9, and (f) PDDA/PAA grown at pH 3 ( $M_w$  of PAA is 15 000).

It is instructive to compare the average height of the protrusions seen by AFM to the ellipsometric thickness. This comparison is possible only when a reference plane is detectable in the AFM images. Such planes are easy to find for the images in Figure 6c,f. Standard image analysis then provides average heights of 4.3 and 44.2 nm for the protrusions in Figure 6c,f, covering relative surface fractions of 0.26 and 0.4, respectively. When averaged over the whole surface of the image, the average heights of the protrusions are thus 1.1 (i.e.,  $4.3 \times 0.26$ ) and 17.7 nm, whereas the ellipsometric thicknesses of the multilayers are 1 and 20.9 nm, respectively. The good agreement between ellipsometric and AFM values confirms that ellipsometry provides a correct estimate of the average amount of adsorbed material, even for such blobby and rough surfaces.

### Conclusions

We have tested the ability of PEO–silane monolayers grafted onto silicon surfaces to resist the growth of LbL polyelectrolyte multilayers using different pairs of polyelectrolytes of varying molar mass and various pH values. Although the PEO–silane monolayers were previously proved to resist protein adsorption,<sup>37</sup> they fail in many cases to prevent the growth of polyelectrolyte multilayers. At pH 3, PEO monolayers exhibit good polyelectrolyte repellency provided that the polyelectrolytes do not bear hydrogen bond-donating moieties. This is the case for PDPA/PSS multilayers, which are efficiently prevented from growing on the PEO–silane layer. By contrast, PAA- or PVBAC-based multilayers grow on the PEO–silane layer because of hydrogen bonding between the ether groups of PEO and the carboxylic acid or hydroxyl groups of polyelectrolytes. At basic pH, PEO monolayers undergo quicker partial hydrolysis. This phenomenon leads to the formation of negatively charged  $\text{SiO}^-$  defects in the monolayers, which then play the role of adsorption sites for the polycation. Once the polycation is adsorbed, multilayer growth ensues. However, because this is defect-driven growth, the

multilayer is not continuous, being formed of blobs or an open network of adsorbed strands. In addition, the molar mass of the polyelectrolyte also plays a key role, with polyelectrolyte chains of larger molar mass adsorbing on a larger number of defects, resulting in increased stability and faster subsequent growth of the multilayer. This also explains why the PEO layers better resist the adsorption of globular proteins than the adsorption of synthetic polyelectrolytes: in a globular protein, the number of amino acids capable of binding to the layer by H bonding or interacting electrostatically with hydrolysis defects is usually much lower than in a synthetic polymer because proteins are not as flexible but are more compact than polyelectrolyte chains. However, when a fibrillar protein such as collagen is used, the PEO–silane layers behave quite similarly to them as to synthetic polyelectrolytes, with nonuniform adsorbed films being formed.<sup>60</sup>

These results show that the proper selection of polyelectrolytes and deposition conditions can lead to the prevention of multilayer deposition on PEO–silane silicon surfaces. However, the range of proper conditions is limited, and much remains to be done to develop more universal polyelectrolyte-repellent surfaces.

**Acknowledgment.** We thank G. Baralia and F. Cecchet for useful discussions about silanation, H. Alem for help with the synthesis of PVBAC, and P. Rouxhet for access to XPS. Financial support was provided by the Belgian National Fund for Scientific Research, the French Community of Belgium (ARC Dynanome), the Wallonia Region (Nanosens project), the Belgian Federal Public Planning Service Science Policy (Inter-University Attraction Poles FS<sup>2</sup>), and the Belgian Fund for Collective Fundamental Research (FRFC). B.N. is Research Associate of the Belgian National Funds for Scientific Research (FNRS).

LA701055Y

(60) Denis, F. A.; Pallandre, A.; Nysten, B.; Jonas, A. M.; Dupont-Gillain, C. *Small* **2005**, *1*, 984.